Experimental and Molecular Pathology 110 (2019) 104279

Contents lists available at ScienceDirect

Experimental and Molecular Pathology

journal homepage: www.elsevier.com/locate/yexmp

miR-149-5p protects against high glucose-induced pancreatic beta cell apoptosis via targeting the BH3-only protein BIM

Dongyun Ruan[a,1], Yanfeng Liu[a,1], Xiaoqing Wang[b], Dahao Yang[b], Yan Sun[c,*]

[a] Department of Cardiology, Jiangxi Provincial People's Hospital Affiliated to Nanchang University, Nanchang, China
[b] Department of Cardiology, Fuwai Hospital, Chinese Academy of Medical Sciences, Shenzhen, China
[c] Department of Endocrinology, Hospital of Southern University of Science and Technology, Shenzhen, China

ARTICLE INFO

Keywords:
Diabetes mellitus
miR-149-5p
Cell apoptosis
Insulin secretion
ROS production
BIM

ABSTRACT

Diabetes mellitus (DM) is characterized by the elevated blood glucose levels and is regarded as one of the most threatening diseases worldwide. The dysfunction of pancreatic beta cells is a key contributor for the pathophysiology of DM. There is growing evidence showing the role of microRNAs (miRNAs) in the regulation of pancreatic beta cell functions. In the present study, we determined the expression of miR-149-5p in pancreatic beta cells under high-glucose (HG) stimulation and explored the underlying mechanism of miR-149-5p-mediated functions of pancreatic beta cells. The results showed the down-regulation of miR-149-5p in the pancreatic beta cell line (MIN6 cells) under HG stimulation. Overexpression of miR-149-5p protected against HG-induced cell apoptosis and impairment of insulin secretion, and attenuated HG-induced an increase in reactive oxygen species (ROS) production in MIN6 cells; while inhibition of miR-149-5p suppressed cell viability, induced cell apoptosis, inhibited insulin secretion and enhanced ROS production in MIN6 cells. Further mechanistic studies revealed that miR-149-5p targeted the BH3-only protein BIM 3′ untranslated region and suppressed BIM expression in MIN6 cells. The rescue experimental assays showed that enforced expression of BIM attenuated the miR-149-5p-mediated effects in HG-stimulated pancreatic beta cells. In conclusion, the present study for the first time elucidated the biological functions of miR-149-5p in regulating pancreatic beta cell functions. The data from the present study provided evidence showing that miR-149-5p protected against HG-induced pancreatic beta cell apoptosis partly via suppressing BIM expression. The therapeutic potential of miR-149-5p in the treatment of DM still requires further detailed investigations.

1. Introduction

Diabetes mellitus (DM) is characterized by the elevated blood glucose levels and is regarded as one of the most threaten diseases worldwide (Ceriello et al., 2019; Jaacks et al., 2019). Due to the large population affected by DM, DM has become a serious public health problem and imposed heavy social burdens (Klatman et al., 2019). Up to date, various breaking through findings regarding the pathophysiology of DM have been revealed, however, the detailed mechanisms of DM remains under-studied. As far as we know, the dysfunction and loss of pancreatic beta cells that leads to the insufficient insulin secretion have been identified as the key factors in the pathogenesis of type 2 DM (Chen et al., 2017a). Studies have demonstrated that hyperglycemia is one of main contributors that induce pancreatic beta cell apoptosis and impair insulin secretion (Boland et al., 2017). In the aspect of clinical management, maintaining the normal glucose level and homeostasis is the main therapeutic strategy. The protection and improvement of the functional pancreatic beta cells have been intensively studied due to the regulatory role of these cells in maintaining glucose homeostasis (Frank et al., 2018). Unfortunately, the underlying mechanisms of the dysfunctional pancreatic beta cells remain elusive, which require further scientific investigations.

MicroRNAs (miRNAs) are a class of endogenous small non-coding RNAs and have ~21 nucleotides in length. MiRNAs exerted their regulatory actions by binding to the 3′ untranslated regions (3’UTRs) or the coding regions of mRNAs, which induce the degradation of the targeted mRNAs (Hashimoto and Tanaka, 2017). MiRNAs have been found to play important roles in various diseases such as cancer, neurodegenerative diseases, cardiovascular diseases and DM (Paul et al., 2018). The involvement of the miRNAs in the pathophysiology of DM has been

---

[*] Corresponding author at: Department of Endocrinology, Hospital of Southern University of Science and Technology, Shenzhen 518055, China.
E-mail address: sunyanendo@yandex.com (Y. Sun).

[1] Both authors equally contributed to this work.

https://doi.org/10.1016/j.yexmp.2019.104279
Received 30 March 2019; Received in revised form 25 June 2019; Accepted 27 June 2019

demonstrated in a line of studies. For examples, miR-204 was found to control the glucagon-like peptide 1 receptor expression, which affects the insulin secretion of pancreatic beta cells (Jo et al., 2018). Song et al., showed that circulating miR-375 served as a biomarker of pancreatic beta cell death, and exerted protective effects on the beta cell mass (Song et al., 2017). Wang et al., found that miR-92a exerted protective actions in the pancreatic beta cells by targeting Kruppel-like factor 2 in DM (Wang et al., 2018). Recently, miR-149-5p were downregulated by cytokines in type 1 DM (Grieco et al., 2017). Furthermore, miR-149-5p was also found to attenuate the hyperglycemia-induced expression of tumor necrosis factor-alpha and endoplasmic reticulum stress markers (Yuan et al., 2017). However, the role of miR-149-5p in regulating the functions of pancreatic beta cells remains unknown.

Based on the evidence from previous studies, we speculated that miR-149-5p could regulate the function of pancreatic beta cells. In this study, we determined the expression of miR-149-5p in pancreatic beta cells under high glucose (HG) conditions and explored the underlying mechanism of miR-149-5p-mediated functions of pancreatic beta cells. The present study aimed to advance our knowledge into understanding the role of miR-149-5p in pancreatic beta cell functions.

2. Materials and methods

2.1. Cell culture and high glucose stimulation

The pancreatic beta cell line (MIN6 cells) were purchased from ATCC (CRL-11506, Manassas, USA). The MIN6 cells were cultured in the Dulbecco's Modified Eagle's Medium (DMEM with 5.5 mM glucose; #D6064, Sigma, St. Louis, USA) supplemented with 10% fetal bovine serum (FBS; Gibco, Waltham, USA). The MIN6 cells were maintained in a humidified incubator with 5% CO_2 at 37 °C. For the high glucose stimulation, the MIN6 cells were incubated in the full medium containing 25 mM glucose (final concentration in the medium) for the indicated time durations.

2.2. MiRNAs, plasmids and cell transfections

The miRNA oligonucleotides including miR-149-5p mimics (5′-UCUGGCUCCGUGUCUUCACUCCC-3′), miR-149-5p inhibitors (5′-GGGAGUGAAGACACGGAGCCAGA-3′) and their respective scrambled negative controls (NC): mimics NC (5’-UUCUCCGAACGUGUCACG UTT-3′) or inhibitors NC (5′-CAGUACUUUUGUGUAGUACAA-3′) were all obtained from Ribobio (Guangzhou, China). The plasmid constructs that overexpress BH3-only protein BIM was generated by cloning the BIM into the pcDNA3.1 vector, and pcDNA3.1 was used as the corresponding NC (GenePharma, Shanghai, China). The effective cell transfections with miRNAs or plasmids were performed by Lipofectamine 3000 reagent (Thermo Fisher Scientific, Waltham, USA) according to the manufacturer's instructions, and the transfected cells were collected for further assays at 24 h after transfection.

2.3. Quantitative real-time PCR (qRT-PCR)

Total RNA from treated MIN6 cells was extracted using a RNeasy RNA Mini Kit (QIAGEN, Hilden, Germany). RNA samples were reverse transcribed using the miScript Reverse Transcriptase Kit (Takara, Dalian, China), and the qRT-PCR analysis was performed in an ABI7900 Real-time PCR System (Applied Biosystems, Foster City, USA) using SYRB Green Master Mix kit (Takara). U6 was used as the internal control for miR-149-5p expression, and glyceraldehyde-3-phosphate dehydrogenase was used as internal control for BIM mRNA expression. The relative expression of detected genes was calculated using $2^{-\Delta\Delta Ct}$ formula. The primers for real-time PCR were shown in supplemental Table S1.

2.4. Apoptosis assay

The cell apoptotic rates of treated MIN6 cells were detected using the Annexin V/ propidium iodide (PI) Apoptosis Detection kit (Thermo Fisher Scientific, Waltham, USA). Briefly, the treated MIN6 cells were harvested followed by incubated with annexin V (25 ng/ml) and 10 mg/ml PI for 15 min in the dark environment at room temperature. After incubation, the apoptotic rates of the stained cells were measured using flow cytometry (BD Biosciences, San Jose, USA).

2.5. Insulin secretion assay

The secreted insulin levels in the medium from the treated MIN6 cells were detected using a commercial Insulin ELISA kit (Thermo Fisher Scientific). Briefly, the medium of treated MIN6 cells was collected for insulin measurement. To determine total insulin content, MIN6 cells were subjected to sonication in acid methanol (2% H_2SO_4) followed by centrifugation at 12000*g* for 10 min at 4 °C. After centrifugation, the supernatant was collected for the measurement of insulin levels. The insulin levels were determined using the Insulin ELISA kit (Thermo Fisher Scientific) according to the manufacturer's protocol. The secreted insulin level in the medium was normalized by the level of total insulin content.

2.6. Reactive oxygen species (ROS) production

For the ROS production, the treated MIN6 cells were plated on a 6-well plate and were further cultured for 24 h. After that, the MIN6 cells were incubated with 10 μM DCFH-DA (Cell Biolabs, lnc., San Diego, USA) for 30 min at 37 °C. The intracellular ROS production was assessed by measuring the fluorescent signaling under a fluorescence microscopy (Olympus, Tokyo, Japan). The intensity of the fluorescent signals was analyzed using Image J software (https://imagej.nih.gov/ij/).

2.7. Caspase-3 activity

The caspase-3 activity of the treated MIN6 cells was measured using a commercial caspase-3 activity assay kit (Roche, Basel, Switzerland) according to the manufacturer's instructions (Lin et al., 2014).

2.8. Cell counting kit-8 (CCK-8) assay

Cell viability of treated MIN6 cells was examined by the CCK-8 assay kit (Beyotime, Beijing, China). Briefly, treated MIN6 cells were plated onto a 96-well plate, after 48 h further culture, the MIN6 cells were subjected to incubate with CCK-8 solution for 1 h at 37 °C. After incubation, the MIN6 cell viability was determined by measuring the optical density at a wavelength of 450 nm on a microplate reader (Bio-Tek, Winooski, USA).

2.9. Protein extraction and western blot assay

The treated MIN6 cells were collected following by washing with ice-cold phosphate-buffered saline twice, and the MIN6 cells were lysed by incubating with the ice-cold RIPA buffer with protease inhibitors (Sigma) for 15 min. The cell lysates were centrifuged at 12000 *g* for 10 min at 4 °C and supernatant was collected as protein samples. Equal amounts of the proteins were solved on a 10% SDS-PAGE and were then transferred to the polyvinylidene fluoride membranes (Sigma). The membranes were then blocked with 5% non-fat milk for 1 h at room temperature and subsequently incubated with the corresponding primary antibodies for pro- and cleaved caspase-3 (1:1000, #9662, Cell Signaling Technology, Danvers, USA), pro- and cleaved caspase-9 (1:1000, #9508, Cell Signaling Technology), BIM (1:1000, #2819, Cell Signaling Technology) and β-actin (1:1000, #4967, Cell Signaling Technology) overnight at 4 °C. After washing, the membranes were again incubated with corresponding secondary antibodies with horseradish peroxidase conjugated (Cell Signal Technology). The protein blots were detected using the enhanced chemiluminescence kit (Thermo Fisher Scientific) by following the manufacturer's instructions.

2.10. *Luciferase reporter assay*

The luciferase reporter was used to determine interaction between miR-149-5p and BIM 3’UTR. Briefly, the fragment of the wild-type (WT) BIM 3’UTR containing the putative miR-149-5p binding site or the corresponding mutant (MUT) BIM 3’UTR was amplified and subcloned into the pmirGLO luciferase reporter vector (Promega, Madison, USA). For the detection of luciferase activity, MIN6 cells were co-transfected with different miRNAs (mimics NC, miR-149-5p mimics, inhibitors NC or miR-149-5p inhibitors) and luciferase reporter vectors (pmirGLO-BIM 3’UTR-WTor pmirGLO-BIM 3’UTR-mutant), and at 48 h after co-transfection, the luciferase activity was assessed using a Dual-Luciferase Reporter Assay kit (Promega) according to the manufacturer's instructions.

2.11. *Statistical analyses*

All the in vitro assays were performed independently for 3 times, and the data were presented as mean ± standard deviation. The statistical analyses were performed using GraphPad Prism 5.0 (GraphPad Software Lin., La Jolla, USA). The statistical significance for comparing data between two groups was analyzed by Student's *t*-test; the statistical significance for comparing data among multiple groups was analyzed by one-way analysis of variance followed by Bonferroni's post-hoc test. $P < .05$ was considered statistically significant.

3. Results

3.1. *Effects of HG treatment on cell viability, caspase-3 activity and miR-149-5p expression in MIN6 cells*

Firstly, we tested the effects of HG treatment for different periods on cell viability and caspase-3 activity, and the CCK-8 assay and caspase-3 activity assay results showed that HG treatment for 6, 12 and 24 h suppressed cell viability and increased caspase-3 activity in MIN6 cells, and the effects were in a time-dependent manner (Fig. 1A and B). Furthermore, HG stimulation also time-dependently induced the down-regulation of miR-149-5p in MIN6 cells (Fig. 1C). HG stimulation for 24 h exerted the maximal effects and 24 h treatment duration was selected in the subsequent studies.

3.2. *Effects of miR-149-5p overexpression on cell viability, cell apoptosis, insulin secretion and ROS production in HG-stimulated MIN6 cells*

As miR-149-5p was down-regulated in the HG-stimulated MIN6 cells, we are interested in seeing if restoring or overexpressing miR-149-5p could prevent against the HG-mediated effects in MIN6 cells. The overexpression of miR-149-5p was observed in MIN6 cells with miR-149-5p mimics transfection (Fig. 2A). As expected, HG stimulation for 24 h suppressed cell viability and increased caspase-3 activity, and the effects were significantly attenuated by the presence of miR-149-5p mimics (Fig. 2B and C). The flow cytometry results showed that HG treatment for 24 h significantly increased the cell apoptotic rates, and overexpression of miR-149-5p inhibited the cell apoptosis induced by HG stimulation in MIN6 cells (Fig. 2D). Moreover, by examining the apoptosis-related proteins, we found that HG-stimulation increased the protein levels of cleaved capase-3, and − 9, and decreased the protein level of pro-caspase-3 and -9 in MIN6 cells, and this action was prevented by miR-149-5p overexpression (Fig. 2E). The insulin secretion was determined by ELISA assay, and HG stimulation suppressed the insulin secretion of MIN6 cells, and miR-149-5p mimics transfection

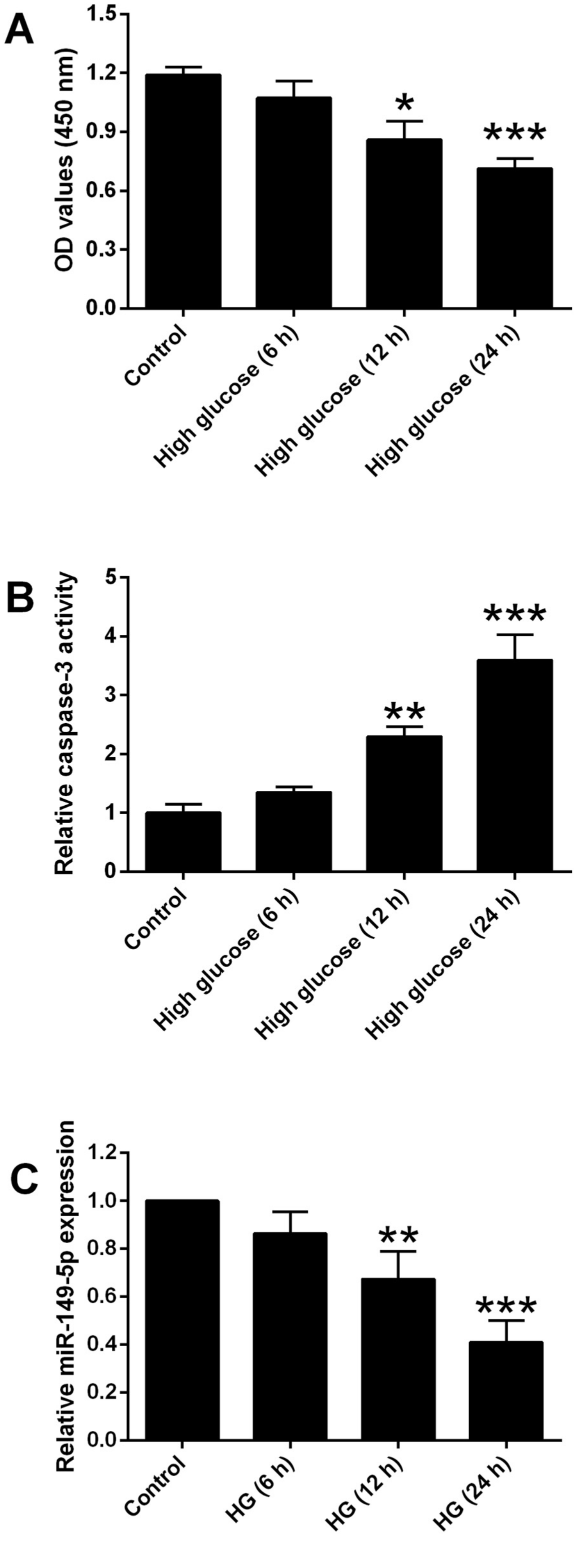

Fig. 1. Effects of HG treatment on cell viability, caspase-3 activity and miR-149-5p expression in MIN6 cells. A: Cell viability was evaluated by CCK-8 assay in MIN6 cells after exposure to HG for 6, 12 and 24 h, respectively. B: Capase-3 activity in MIN6 cells after exposure to HG for 6, 12 and 24 h, respectively. C: MiR-149-5p expression (relative to U6) as determined by qRT-PCR in MIN6 cells after exposure to HG for 6, 12 and 24 h, respectively. $N = 3$; significant differences compared to control group were presented as $^{*}P < .05$, $^{**}P < .01$ and $^{***}P < .001$.

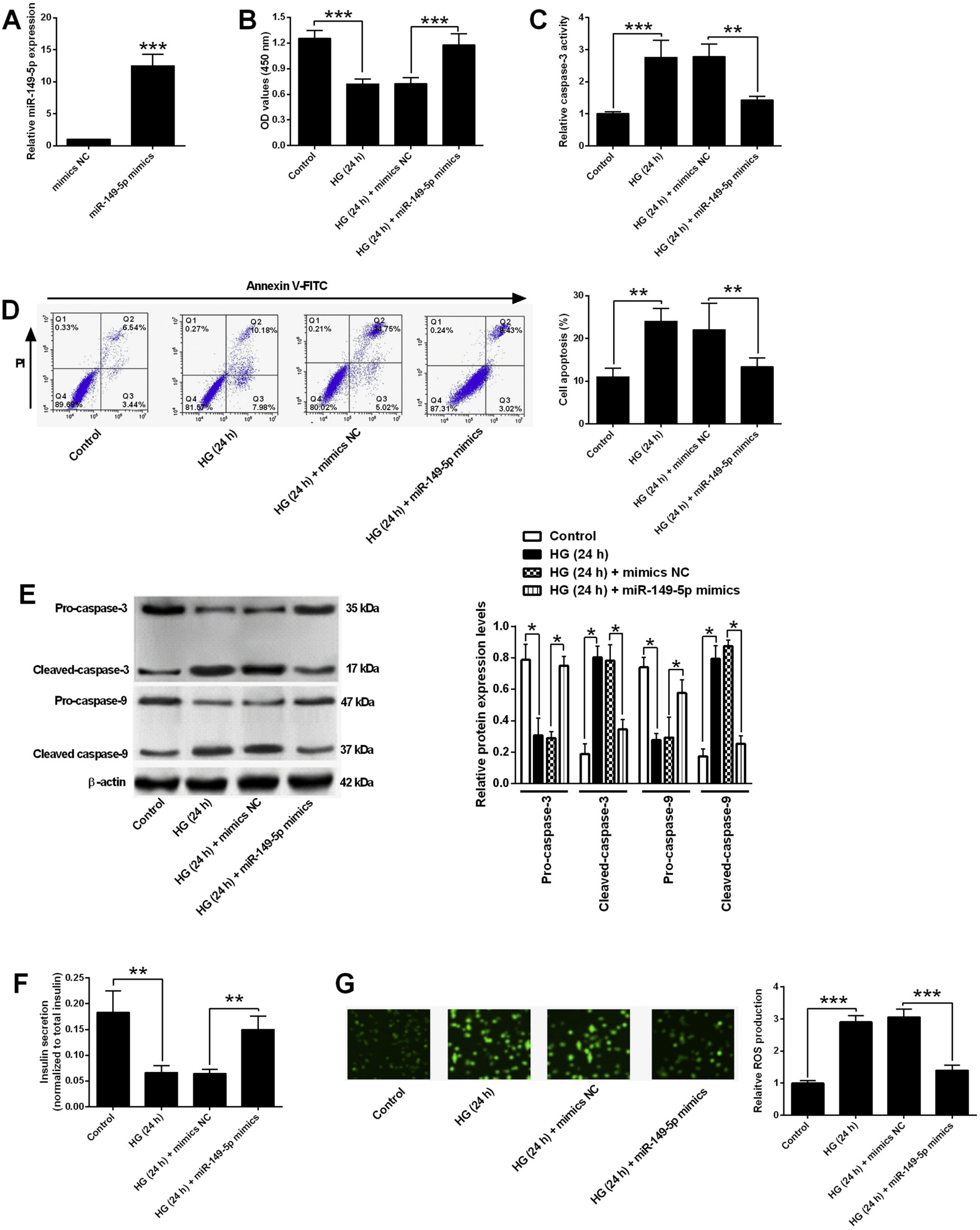

(caption on next page)

Fig. 2. Effects of miR-149-5p overexpression cell viability, cell apoptosis, insulin secretion and ROS production in HG-stimulated MIN6 cells. A: MiR-149-5p expression (relative to U6) as determined by qRT-PCR in MIN6 cells transfected with miR-149-5p mimics or mimics NC. B-E: Effects of miR-149-5p overexpression on cell viability, caspase-3 activity, cell apoptosis and protein levels of apoptosis-related factors in HG-stimulated MIN6 cells as determined by CCK-8 assay, caspase-3 activity assay, flow cytometry and western blot assay, respectively. F: Effects of miR-149-5p overexpression on insulin secretion as determined by ELISA assay in HG-stimulated MIN6 cells. G: Effects of miR-149-5p overexpression on ROS production in HG-stimulated MIN6 cells. $N = 3$; significant differences among different treatment groups were presented as $^{*}P < .05$, $^{**}P < .01$ and $^{***}P < .001$.

increased the insulin secretion in the HG-stimulated MIN6 cells (Fig. 2F). In addition, HG-stimulation also exhibited an enhanced effect on the ROS production in the MIN6 cells, and the HG-induced increase in ROS production was reduced by the overexpression of miR-149-5p (Fig. 2G).

3.3. *Effects of miR-149-5p inhibition on cell viability, cell apoptosis, insulin secretion and ROS production in MIN6 cells*

The inhibition of miR-149-5p was observed in MIN6 cells with miR-149-5p inhibitors transfection when compared to inhibitors NC group (Fig. 3A). The CCK-8, caspase-3 activity and flow cytometry assays showed that inhibition of miR-149-5p suppressed cell viability, increased caspase-3 activity and induced cell apoptosis in MIN6 cells (Fig. 3B–D). In addition, miR-149-5p knockdown significantly increased the proteins levels of cleaved caspase-3 and -9, but decreased the protein levels of pro-caspase-3 and -9 (Fig. 3E). MiR-149-5p knockdown also significantly suppressed the insulin secretion and caused an increase in the ROS production of MIN6 cells (Fig. 3F and G).

3.4. *MiR-149-5p suppressed targeted BIM 3'UTR and suppressed BIM expression*

To find out the downstream targets of miR-149-5p, we performed the bioinformatics prediction using TargetScan tool. Among the predicted targets, BIM was selected for further detailed examination because of its role in regulating cell viability and cell apoptosis. As shown in Fig. 4A, the miR-149-5p formed the imperfect bindings with the BIM 3'UTR (position 475–481, conserved), and the WT and MUT fragments of BIM 3'UTR was cloned into the pmirGLO vector. As shown in Fig. 4B, overexpression of miR-149-5p exerted inhibitory effects on the luciferase activity of WT reporter vector, while knockdown of miR-149-5p increased the luciferase activity. However, miR-149-5p had no effects on the luciferase activity when the reporter vectors containing the MUT BIM 3'UTR (Fig. 4C). The qRT-PCR and western blot assays further showed that miR-149-5p overexpression down-regulated BIM expression in MIN6 cells; while miR-149-5p knockdown up-regulated BIM expression in MIN6 cells (Fig. 4D and E). As expected, HG stimulation for 24 h caused an increase in the BIM expression; and the presence of miR-149-5p mimics attenuated the enhanced effects of HG-stimulation on BIM expression in MIN6 cells (Fig. 4F and G).

3.5. *Overexpression of BIM attenuated the effects of miR-149-5p overexpression on cell viability, cell apoptosis, insulin secretion and ROS production in HG-stimulated MIN6 cells*

To further confirm the involvement of BIM in the miR-149-5p-mediated effects in the MIN6 cells, we performed the rescue experiments by enforced expression of BIM, and the enforced upregulation of BIM was achieved via transfecting MIN6 cells with pcDNA3.1-BIM (Fig. 5A and B). Overexpression of BIM markedly suppressed cell viability and increased caspase-3 activity in MIN6 cells under normal glucose and HG conditions (see Supplemental Fig. S1). In terms of cell viability, caspapse-3 activity and cell apoptosis, enforced expression of BIM attenuated the enhanced effects of miR-149-5p overexpression on cell viability, and reversed the inhibitory effects of miR-149-5p overexpression on caspase-3 activity as well as cell apoptosis (Fig. 5C–E), moreover, prevented the miR-149-5p-induced changes in the expression level of apoptosis-related proteins in the MIN6 under the condition of HG stimulation (Fig. 5F). In terms of insulin secretion and ROS production, miR-149-5p consistently increased insulin secretion and suppressed ROS production in HG-stimulated MIN6 cells, and the effects were attenuated by enforced BIM expression in HG-stimulated MIN6 cells (Fig. 5G and H).

4. Discussion

The dysfunction of pancreatic beta cells is a key contributor for the pathophysiology of DM, and understanding the molecular mechanisms underlying the dysfunction of pancreatic beta cells would be helpful us to identify novel therapeutic targets for a better treatment of DM. Recently, many miRNAs have been identified for their involvement in the pancreatic beta cell functions. In the present study, we confirmed the down-regulation of miR-149-5p in the MIN6 cells under HG stimulation. Overexpression of miR-149-5p protected against HG-induced cell death and impairment of insulin secretion and attenuated the HG-induced increase in ROS production in MIN6 cells; while inhibition of miR-149-5p suppressed cell viability, increased cell apoptosis, suppressed insulin secretion and enhanced ROS production in MIN6 cells. Further mechanistic studies revealed that miR-149-5p targeted the BIM 3'UTR and suppressed the expression of BIM in MIN6 cells. The rescue experimental assays showed enforce expression of BIM attenuated the miR-149-5p-mediated effects in HG-stimulated pancreatic beta cells. Collectively, our data for the first time demonstrated the role of miR-149-5p in regulating pancreatic beta cell apoptosis via targeting BIM.

So far, the role of miR-149-5p has been investigated in various studies. In most cancer studies, miR-149-5p was demonstrated to play as a tumor suppressor in various types of cancers including hepatocellular carcinoma (Ji et al., 2019), non-small cell lung cancer (Li et al., 2018), osteosarcoma (Xu et al., 2018), nasopharyngeal carcinoma (Kong et al., 2018) and melanoma (Chen et al., 2017b); while studies from Tian et al., suggested the oncogenic role and anti-apoptotic effects of miR-149-5p in acute myeloid leukemia (Tian and Yan, 2016). The discrepancy may be due to the different types of cancer cells. In cardiovascular disease, miR-149-5p could promote efferocytosis in advanced atherosclerosis (Ye et al., 2019). The dysregulation of miR-149-5p was identified in the insulin resistance mice (Zhao et al., 2019). MiR-149-5p was found to be down-regulated by cytokines and has been implicated for its role in attenuating beta cell apoptosis (Grieco et al., 2017). Evidence from studies using endothelial cells showed that miR-149-5p was also found to attenuate the hyperglycemia-induced expression of tumor necrosis factor-alpha and endoplasmic reticulum stress markers (Yuan et al., 2017). In our study, we further identified the up-regulation of miR-149-5p in pancreatic beta cells upon HG stimulation, and overexpression of miR-149-5p protected HG-induced dysfunctions of pancreatic beta cells; while inhibition of miR-149-5p induced pancreatic beta cell dysfunctions including suppressed cell viability, increased cell apoptosis and ROS production as well as impaired insulin secretion. These data suggest that miR-149-5p played a protective role in the functions of pancreatic beta cells.

The downstream targets of miR-149-5p were further predicted using the online TargetScan tool, and BIM was selected for further investigations. The interactions between miR-149-5p and BIM were further confirmed by luciferase reporter assay, and qRT-PCR and western blot assay also showed that miR-149-5p negatively regulated BIM expression in MIN6 cells. BIM is a novel member of the Bcl-2 family and is

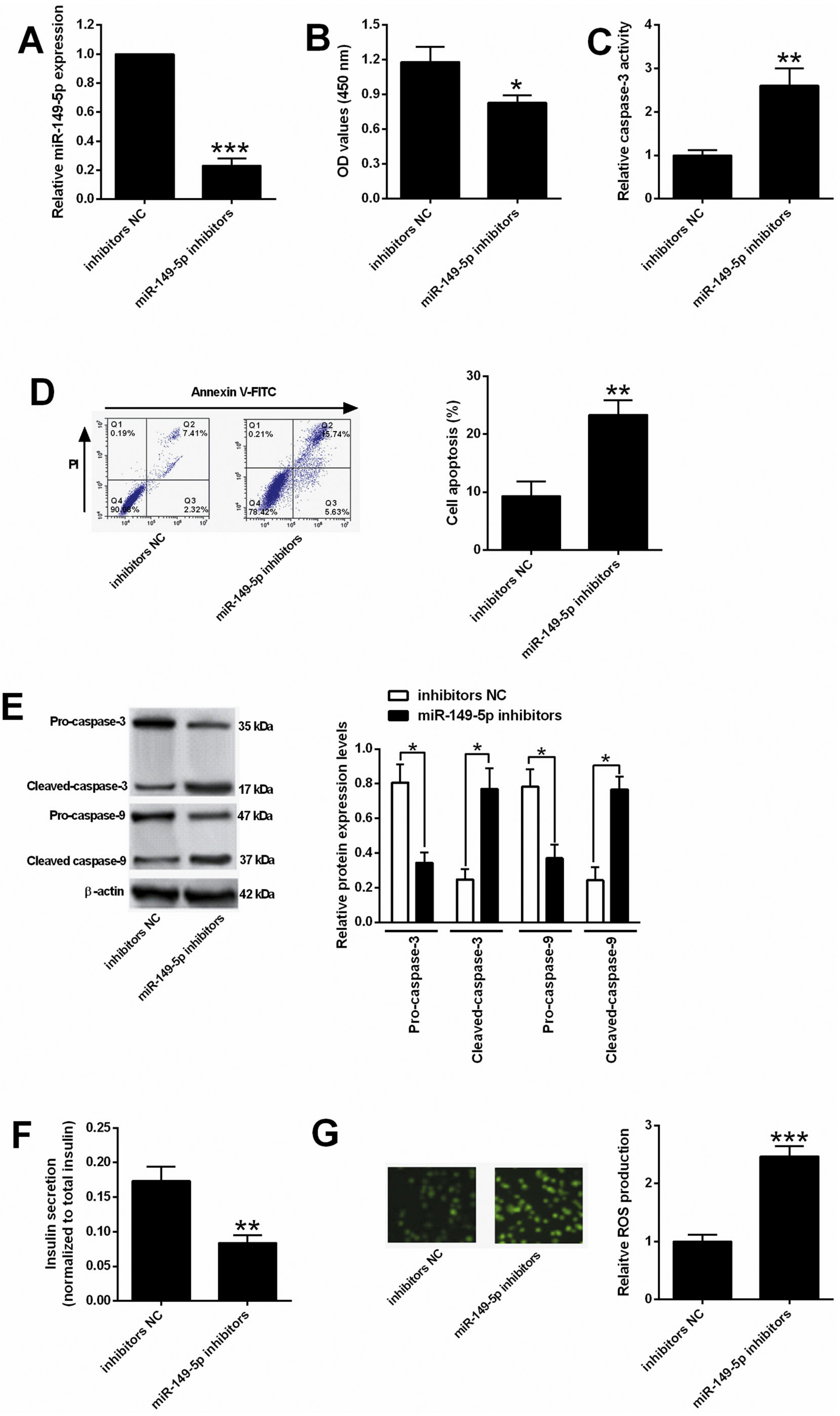

(caption on next page)

Fig. 3. Effects of miR-149-5p inhibition on cell viability, cell apoptosis, insulin secretion and ROS production in MIN6 cells. A: MiR-149-5p expression (relative to U6) as determined by qRT-PCR in MIN6 cells transfected with miR-149-5p inhibitors or inhibitors NC. B-D: Effects of miR-149-5p inhibition on cell viability, increased caspase-3 activity and induced cell apoptosis in MIN6 cells as determined by CCK-8, caspase-3 activity assay, and flow cytometry respectively. E: Effects of miR-149-5p on the protein expression levels of pro- and cleaved caspase-3, and pro- and cleaved caspase-9 in MIN6 cells. F: Effects of miR-149-5p knockdown on insulin secretion in MIN6 cells as determined by ELISA assay. G: Effects of miR-149-5p knockdown on increased the ROS production in MIN6 cells. N = 3; significant differences among different treatment groups were presented as *P < .05, **P < .01 and ***P < .001.

an important pro-apoptotic factor that initiates the apoptotic processes (O'Connor et al., 1998). Studies by McKenzie et al., showed that pancreatic islet cell apoptosis induced by glucose was mediated via BIM (McKenzie et al., 2010). BIM was induced by pro-inflammatory cytokines, which contributed to the beta cell death and the mitochondrial generation of ROS (Mehmeti et al., 2011). Recently, Tennant et al., also showed that inhibition of Myt3 could sensitize islet cells to HG-induced cell death via upregulation of BIM (Tennant et al., 2016). On the other hand, BIM could be targeted by different miRNAs such as miR-92a (Oda et al., 2018), miR-19b (Baumgartner et al., 2018), miR-24 (Feng et al., 2017) and so on, and the suppression of BIM by these miRNAs contributed to the anti-apoptotic effects in different types of cells. In agreement of previous studies, our data showed that BIM was upregulated in pancreatic beta cells under the HG stimulation, and this effect could be reversed by miR-149-5p overexpression. More importantly, the rescue experiments further showed that enforced expression of BIM impaired the protective effects of miR-149-5p on HG-stimulated pancreatic beta cells. Collectively, these data may imply that miR-149-5p exerted its protective effects on HG-stimulated pancreatic beta cells likely via targeting BIM.

5. Conclusions

In conclusion, the present study for the first time elucidated the biological functions of miR-149-5p in regulating pancreatic beta cell functions. The data from the present study provided evidence showing

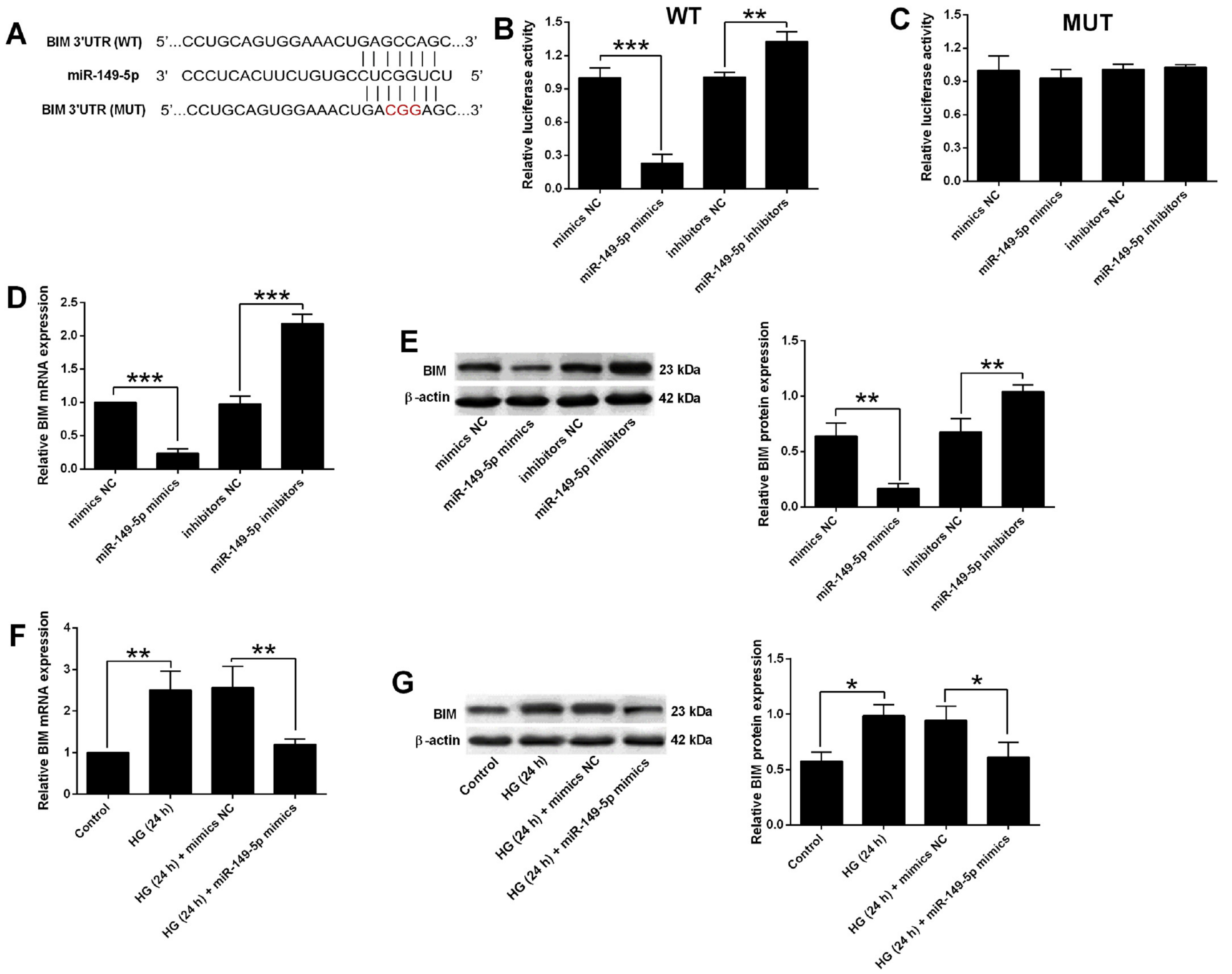

Fig. 4. MiR-149-5p targeted BIM 3'UTR and suppressed BIM expression. A: Putative binding sites between miR-149-5p and BIM. B-C: Relative luciferase activity as determined by luciferase reporter assay in MIN6 cells after being co-transfected with different miRNAs and WT/MUT luciferase reporter vectors. D-E: The expression levels of BIM mRNA (relative to GAPDH) and protein as determined by qRT-PCR and western blot, respectively, were assessed in MIN6 cells after being transfected with different miRNAs. F-G: Effects of miR-149-5p overexpression on the expression of BIM in HG-stimulated MIN6 cells. N = 3; significant differences among different treatment groups were presented as **P < .01 and ***P < .001.

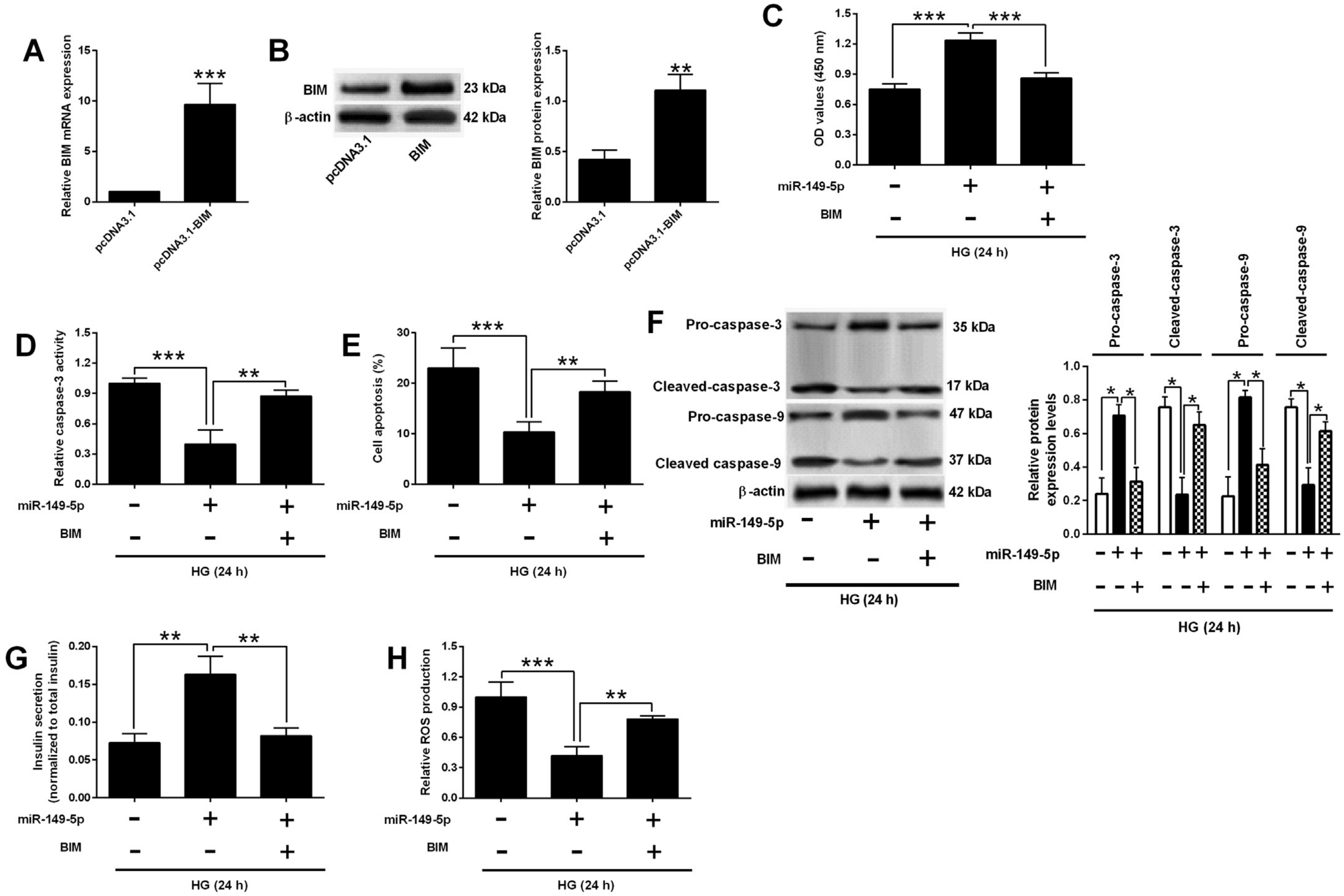

Fig. 5. Effects of BIM overexpression on cell viability, cell apoptosis, insulin secretion and ROS production in HG-stimulated MIN6 cells with miR-149-5p overexpression. A-B: The expression of BIM mRNA (relative to GAPDH) and protein was determined in MIN6 cells after being transfected with pcDNA3.1-BIM or pcDNA3.1. C-E: Effects of BIM overexpression on cell viability, caspase-3 activity and cell apoptosis in HG-stimulated MIN6 cells with miR-149-5p overexpression. F: Effects of BIM overexpression on the protein expression levels of pro- and cleaved caspase-3, and pro- and cleaved caspase-9 in HG-stimulated MIN6 cells with miR-149-5p overexpression. G: Effects of BIM overexpression on insulin secretion in HG-stimulated cells with miR-149-5p overexpression. H: Effects of BIM overexpression on the ROS production in HG-stimulated cells with miR-149-5p overexpression. N = 3; significant differences among different treatment groups were presented as $*P < .05$, $**P < .01$ and $***P < .001$.

that miR-149-5p protected against HG-induced pancreatic beta cell apoptosis partly via suppressing BIM expression. The therapeutic potential of miR-149-5p in the treatment of DM still requires further detailed investigations.

Supplementary data to this article can be found online at https://doi.org/10.1016/j.yexmp.2019.104279.

Funding

This study was supported by the Science and Technology project of Shenzhen City of China (JCYJ20170413114916687 and JCYJ20180306170650122).

Declaration of Competing Interest

None.

References

Baumgartner, U., et al., 2018. miR-19b enhances proliferation and apoptosis resistance via the EGFR signaling pathway by targeting PP2A and BIM in non-small cell lung cancer. Mol. Cancer 17, 44.
Boland, B.B., et al., 2017. The dynamic plasticity of insulin production in beta-cells. Mol Metab. 6, 958–973.
Ceriello, A., et al., 2019. Glycaemic variability in diabetes: clinical and therapeutic implications. Lancet Diabetes Endocrinol. 7, 221–230.
Chen, C., et al., 2017a. Human beta cell mass and function in diabetes: recent advances in knowledge and technologies to understand disease pathogenesis. Mol Metab. 6, 943–957.
Chen, W., et al., 2017b. The negative regulation of miR-149-5p in melanoma cell survival and apoptosis by targeting LRIG2. Am. J. Transl. Res. 9, 4331–4340.
Feng, Z., et al., 2017. Mir-24 regulates hepatocyte apoptosis via BIM during acute liver failure. Am. J. Transl. Res. 9, 4925–4935.
Frank, J.A., et al., 2018. Optical tools for understanding the complexity of beta-cell signalling and insulin release. Nat Rev Endocrinol. 14, 721–737.
Grieco, F.A., et al., 2017. MicroRNAs miR-23a-3p, miR-23b-3p, and miR-149-5p regulate the expression of proapoptotic BH3-only proteins DP5 and PUMA in human pancreatic beta-cells. Diabetes 66, 100–112.
Hashimoto, N., Tanaka, T., 2017. Role of miRNAs in the pathogenesis and susceptibility of diabetes mellitus. J. Hum. Genet. 62, 141–150.
Jaacks, L.M., et al., 2019. The obesity transition: stages of the global epidemic. Lancet Diabetes Endocrinol. 7, 231–240.
Ji, D., et al., 2019. Long non-coding RNA LINC00461/miR-149-5p/LRIG2 axis regulates hepatocellular carcinoma progression. Biochem. Biophys. Res. Commun. 512, 176–181.
Jo, S., et al., 2018. miR-204 controls glucagon-like peptide 1 receptor expression and agonist function. Diabetes 67, 256–264.
Klatman, E.L., et al., 2019. Blood glucose meters and test strips: global market and challenges to access in low-resource settings. Lancet Diabetes Endocrinol. 7, 150–160.
Kong, Y.G., et al., 2018. LncRNA-LINC00460 facilitates nasopharyngeal carcinoma tumorigenesis through sponging miR-149-5p to up-regulate IL6. Gene. 639, 77–84.
Li, J., et al., 2018. LncRNA-PCAT-1 promotes non-small cell lung cancer progression by regulating miR-149-5p/LRIG2 axis. J. Cell. Biochem. https://doi.org/10.1002/jcb.28046. Epub ahead of print.
Lin, X., et al., 2014. Downregulation of Bcl-2 expression by miR-34a mediates palmitate-induced Min6 cells apoptosis. J. Diabetes Res. 2014, 258695.
McKenzie, M.D., et al., 2010. Glucose induces pancreatic islet cell apoptosis that requires

the BH3-only proteins Bim and Puma and multi-BH domain protein Bax. Diabetes. 59, 644–652.

Mehmeti, I., et al., 2011. Modulation of Bcl-2-related protein expression in pancreatic beta cells by pro-inflammatory cytokines and its dependence on the antioxidative defense status. Mol. Cell. Endocrinol. 332, 88–96.

O'Connor, L., et al., 1998. Bim: a novel member of the Bcl-2 family that promotes apoptosis. EMBO J. 17, 384–395.

Oda, T., et al., 2018. Mex-3B induces apoptosis by inhibiting miR-92a access to the Bim-3'UTR. Oncogene. 37, 5233–5247.

Paul, P., et al., 2018. Interplay between miRNAs and human diseases. J. Cell. Physiol. 233, 2007–2018.

Song, I., et al., 2017. Circulating microRNA-375 as biomarker of pancreatic beta cell death and protection of beta cell mass by cytoprotective compounds. PLoS One 12, e0186480.

Tennant, B.R., et al., 2016. Myt3 suppression sensitizes islet cells to high glucose-induced cell death via Bim induction. Cell Death Dis. 7, e2233.

Tian, P., Yan, L., 2016. Inhibition of MicroRNA-149-5p induces apoptosis of acute myeloid leukemia cell line THP-1 by targeting Fas ligand (FASLG). Med. Sci. Monit. 22, 5116–5123.

Wang, W., et al., 2018. MiRNA-92a protects pancreatic B-cell function by targeting KLF2 in diabetes mellitus. Biochem. Biophys. Res. Commun. 500, 577–582.

Xu, R.D., et al., 2018. miR-149-5p inhibits cell growth by regulating TWEAK/Fn14/PI3K/AKT pathway and predicts favorable survival in human osteosarcoma. Int. J. Immunopathol. Pharmacol. 32 (2058738418786656).

Ye, Z.M., et al., 2019. LncRNA MIAT sponges miR-149-5p to inhibit efferocytosis in advanced atherosclerosis through CD47 upregulation. Cell Death Dis. 10, 138.

Yuan, J., et al., 2017. Effect of the diabetic environment on the expression of MiRNAs in endothelial cells: Mir-149-5p restoration ameliorates the high glucose-induced expression of TNF-alpha and ER stress markers. Cell. Physiol. Biochem. 43, 120–135.

Zhao, X., et al., 2019. High-throughput sequencing of small RNAs and analysis of differentially expressed microRNAs associated with high-fat diet-induced hepatic insulin resistance in mice. Genes Nutr. 14, 6.